Journal of Nuclear Materials 386–388 (2009) 323–327

Contents lists available at ScienceDirect

Journal of Nuclear Materials

journal homepage: www.elsevier.com/locate/jnucmat

Fracture toughness master-curve analysis of the tempered martensitic steel Eurofer97

Pablo Mueller [a,*], P. Spätig [a], R. Bonadé [a], G.R. Odette [b], D. Gragg [b]

[a] Fusion Technology-Materials, CRPP-EPFL, Association EURATOM-Confédération Suisse, ODGA-109, 5232 Villigen PSI, Switzerland
[b] Materials and Mechanical Engineering Department, University of California, Santa Barbara, CA 93106-5070, USA

A B S T R A C T

We report fracture toughness data for the reduced activation tempered martensitic steel Eurofer97 in the lower to middle transition region. The fracture toughness was measured from tests carried out on 0.35*T* and 0.87*T* pre-cracked compact tension specimens. The data were first analyzed using the ASTM E1921 standard. The toughness–temperature behavior and scatter were shown to deviate from the ASTM E1921 standard predictions near the lower shelf. Using the method of maximum likelihood, the athermal component of the master-curve was calculated to better fit the data from the lower to the middle transition region. We showed that these master-curve adjustments are necessary to make the T_o values obtained near the lower shelf with 0.35*T* *C*(*T*) specimens consistent with those obtained in the middle transition region with 0.87*T* *C*(*T*) specimens.

1. Introduction

The high-chromium content martensitic steels have been considered as structural candidates for fusion reactors since the late 1970s [1]. While being attractive candidates, neutron irradiation at temperatures below 400–450 °C results in significant shifts of the so-called ductile to brittle transition temperature [2–7]. In order to quantify this so-called embrittlement and other factors that control toughness in the transition region, Odette et al. proposed a systematic and highly efficient approach based upon the master-curve temperature shift method [8,9]. This method extends the American Society for Testing and Materials master-curve standard [10]. Odette et al. [11] also assembled a large fracture toughness database for the IEA heat of F82H made of a variety of specimens sizes and geometries. They showed that, provided the statistical and constraint loss effects on measured toughness are properly accounted for through a physically based local approach of quasi-cleavage, the data are in reasonable agreement with a ASTM master-curve indexed at −98 °C. Recently, Bonadé et al. also applied this local approach on the existing fracture toughness database of Eurofer97 steel to model the toughness–temperature dependence in the transition region [12]. However, Lucon raised recently some concerns related to the applicability of the ASTM E1921 standard for the tempered martensitic steels [13]. Nonetheless, as explicitly mentioned in Section 3.2.1 of the ASTM E1921-03, the temperered martensitic steels fall into the class of 'ferritic' steels for which the standard is applicable. The goal of this study was to analyze a rather large fracture database (174 data points), obtained with sub-sized compact tension specimens tested in the lower to middle transition region of the reduced activation tempered martensitic Eurofer97 steel. The analysis was made within the framework of the ASTM E1921 standard to evaluate the applicability of the master-curve to the Eurofer97 steel and to identify potential issues that may arise.

2. Materials and experimental procedures

The material studied in this work is the reduced activation Eurofer97 steel, heat E83697, 25 mm thick plate, produced by Böhler AG. This steel contains 8.90 wt.% Cr, 0.12 wt.% C, 0.46 wt.% Mn, 1.07 wt.% W, 0.2 wt.% V, 0.15 wt.% Ta, and Fe for the balance. The steel was heat-treated by normalizing at 1253 K for 0.5 h and tempering at 1033 K for 1.5 h.

The static fracture toughness data reported here were obtained with pre-cracked *C*(*T*) specimens. Specimens of three different sizes were tested, having a thickness (crack front) *B* equal to 22, 9 and 4.5 mm, which are here referred to as 0.87*T* *C*(*T*), 0.35*T* *C*(*T*) or 0.18*T* *C*(*T*), respectively. The width *W* of the specimens was equal to 2*B* and they were fatigue pre-cracked until the crack length *a* to specimen width *W* ratio (*a*/*W*) was about 0.5. The tests were performed over the temperature range [−148, −40 °C]. Temperature control was provided by a PID controller equipped with a regulated N_2 gas flow. The results of the fracture toughness tests have been evaluated following the ASTM E1921 standard in terms of K_{Jc}, an elastic–plastic equivalent stress intensity factor derived from the value of the *J* integral at the onset of cleavage fracture, J_c [10]:

* Corresponding author. Tel.: +41 56 310 44 18; fax: +41 56 310 45 29.
E-mail address: pablo.mueller@psi.ch (P. Mueller).

0022-3115/$ - see front matter © 2008 Elsevier B.V. All rights reserved.
doi:10.1016/j.jnucmat.2008.12.122

$$K_{Jc} = \sqrt{J_c E'}, \tag{1}$$

where E' is the plane strain Young's modulus.

3. Statistical analysis method

At different given temperatures in the transition region, a number of specimens were tested to study the intrinsic scatter in the toughness data. The data were analyzed within the framework of statistical brittle fracture models [14,15] that yield, for highly constrained specimens, the cumulative failure probability as a three parameter Weibull distribution:

$$P_f = 1 - \exp\left[-\left(\frac{K_{Jc} - K_{min}}{K_o(T) - K_{min}}\right)^4\right], \tag{2}$$

where K_{min} is a minimum threshold value, usually taken equal to 20 MPa $m^{1/2}$ for ferritic steels, and $K_o(T)$ corresponds to the K_{Jc} value representing the 63.2% cumulative failure probability. The statistical models predict a B-dependence of the form:

$$K_{B_2} = K_{min} + [K_{B_1} - K_{min}]\left(\frac{B_1}{B_2}\right)^{1/4}. \tag{3}$$

Note that this B-scaling was experimentally verified to work fairly well [16]. The effect of in-plane constraint loss on the measured toughness imposes a higher limit of K_{Jc}, the so-called K_{Jc_limit}, below which the measured toughness can be regarded as independent of the ligament length b. K_{Jc_limit} is defined as

$$K_{Jc\_limit} = \sqrt{\frac{E' b \sigma_y}{M}}, \tag{4}$$

where M is a non-dimensional quantity, b is the ligament length and σ_y is the yield stress. The ASTM E1921 requires that $M = 30$ but this value is discussed in the next section in the light of the presented results.

The temperature dependence of the median toughness of 25.4 mm thick specimens (1T) in the transition region of 'ferritic' steels is given by the so-called ASTM master-curve that reads [17]:

$$K_{Jc\_median(1T)} = A + B\exp(C(T - T_o)). \tag{5}$$

T_o is the reference temperature where the median toughness of a 1T specimen is equal to 100 MPa $m^{1/2}$. The ASTM E1921 standard gives $A = 30$, $B = 70$ and $C = 0.019$. We have recently reported [7,18] a toughness behavior in the lower transition region of the Eurofer97 steel that deviates somewhat from Eq. (5). Owing to the large number of data points of this analyzed database, it is possible to fit the coefficients of Eq. (5). In order to keep the master-curve philosophy, we rewrite Eq. (4) as

$$K_{Jc\_median(1T)} = A + (100 - A)\exp(C(T - T_o)). \tag{6}$$

By doing so, we adjust the level of the athermal part of master-curve (A) as well as the shape (C), while keeping the significance of T_o as the index at 100 MPa $m^{1/2}$. The parameters A, C and T_o in Eq. (6) can be obtained by using the method of maximum likelihood. The likelihood function of the Weibull probability density reads:

$$L = \prod_{i=1}^{N} \frac{4(K_{Jc,i} - K_{min})^3}{(K_o(T) - K_{min})^4} \exp\left(-\left(\frac{K_{Jc,i} - K_{min}}{K_o(T) - K_{min}}\right)^4\right). \tag{7}$$

Having a dataset ($K_{Jc,i}$ at T_i), the coefficient A, C and T_o are determined by solving numerically and iteratively the three equations: $\partial \ln L/\partial A = \partial \ln L/\partial C = \partial \ln L/\partial T_o = 0$, which are, respectively,

$$\sum_{i=1}^{n} \frac{(1 - \exp(C(T_i - T_o))}{(K_o - K_{min})} - \sum_{i=1}^{n} \ln(2) \frac{(K_{J,i} - K_{min})^4 (1 - \exp(C(T_i - T_o))}{(K_o - K_{min})^5} = 0, \tag{8a}$$

$$\sum_{i=1}^{n} \frac{\exp(C(T_i - T_o))(T_i - T_o)}{K_o - K_{min}} - \sum_{i=1}^{n} \frac{(K_{J,i} - K_{min})^4 \exp(C(T_i - T_o))(T_i - T_o)}{(K_o - K_{min})^5} = 0, \tag{8b}$$

$$\sum_{i=1}^{n} \frac{\exp(C(T_i - T_o)}{K_o - K_{min}} - \sum_{i=1}^{n} \frac{(K_{J,i} - K_{min})^4 \exp(C(T_i - T_o)}{(K_o - K_{min})^5} = 0 \tag{8c}$$

with $(K_o - K_{min}) = \frac{A - K_{min}}{\ln(2)^{1/4}} + \frac{(100 - A)\exp(C(T - T_o))}{\ln(2)^{1/4}}$.

4. Results and discussion

Eq. (2) was used to draw failure probability diagrams. An example is shown in Fig. 1 for two datasets of measured toughness data at −100 °C obtained with 0.18T and 0.35T $C(T)$ specimens. The rank probability was calculated as $P_f = (i - 0.3)/(n + 0.4)$, i is the rank of the data considered and n the number of points [19]. This probability diagram was constructed by considering K_{min} = 20 MPa $m^{1/2}$. In Fig. 1, a deviation from the expected linear behavior is observed for the 0.18T $C(T)$ specimens at a limit measured toughness of about 90 MPa $m^{1/2}$, which corresponds to a M value (see Eq. (4)) of about 80. This deviation is attributed to constraint loss that results in an increase of the measured toughness. It has to be emphasized that this M value is significantly larger than $M = 30$ recommended in the ASTM E1921 standard. This observation is also consistent with the extensive fracture database of Rathbun et al. [16] who showed that constraint loss begins at relatively low deformation levels, corresponding to $M \approx 200$ for bend bars. In Fig. 2, the measured toughness is plotted versus temperature along with the K_{Jc_limit} lines associated with $M = 80$. The filled symbols correspond to measured toughness on specimens for which the load–displacement curve passed through a maximum and for which the toughness was calculated at the point of fracture. Such specimens underwent a large amount of plasticity and, as a consequence, suffer from significant constraint loss so that the toughness measured on such specimens is not really representative of cleavage tough-

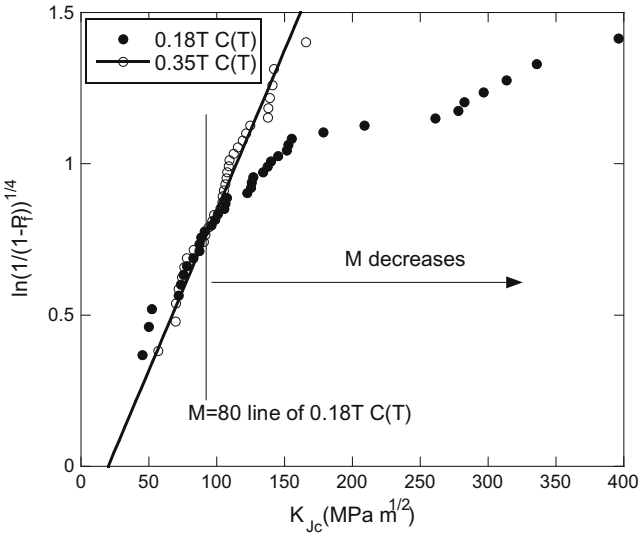

Fig. 1. Failure probability diagram at $T = -100$ °C.

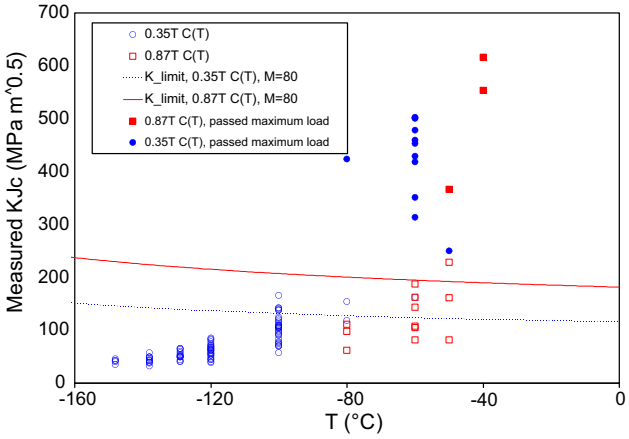

Fig. 2. Measured fracture data and K_{Jc_limit} lines associated with $M = 80$.

ness. Thus, those points were not considered in the following master-curves analysis. In addition, we emphasize that there are in total six datasets, at six different temperatures, that are fully constrained, namely below the K_{Jc_limit} lines associated with $M = 80$. These datasets are the four ones of the 0.35T $C(T)$ specimens at the lowest temperature and the two datasets of the 0.87T $C(T)$ at −80 and −60 °C. These six datasets will be considered later as reference data to assess the shape of the toughness–temperature curve.

First, a multi-temperature determination of T_o was performed according to the ASTM E1921 standard by considering only the 0.87T $C(T)$ data. Note that for the censoring of the data we used a K_{Jc_limit} (Eq. (4)) with $M = 80$. Again, as mentioned above, the three data points that failed after a large amount of plasticity (beyond maximum load on the load–displacement curve) were not considered in the analysis. Only one point lied above the K_{Jc_limit} associated with $M = 80$, which was replaced by the K_{Jc_limit} value according to the standard. T_o was found equal to −78 °C. All 1T-adjusted data are plotted in Fig. 3 along with the MC indexed at −78 °C. One observes that on the lower transition region side, for temperatures $\leqslant$−120 °C, most of the 0.35T $C(T)$ data fall below the median curve. For instance, at −120 °C, only four points over 27 lie above the median curve. However, this temperature is still in the restricted temperature range, defined as $T_o \pm 50$ °C, in which the reference temperature T_o can be in principle determined [10]. Furthermore, in Fig. 4, we plot T_o as determined from a series of

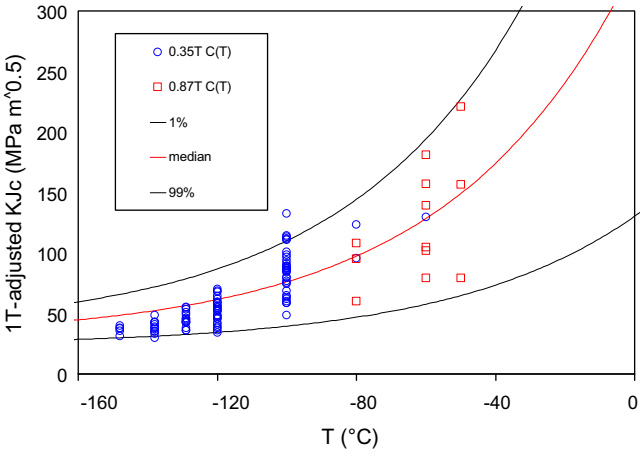

Fig. 3. Standard ASTM E1921 master-curve analysis on the 0.87T $C(T)$ data, T_o = −78 °C.

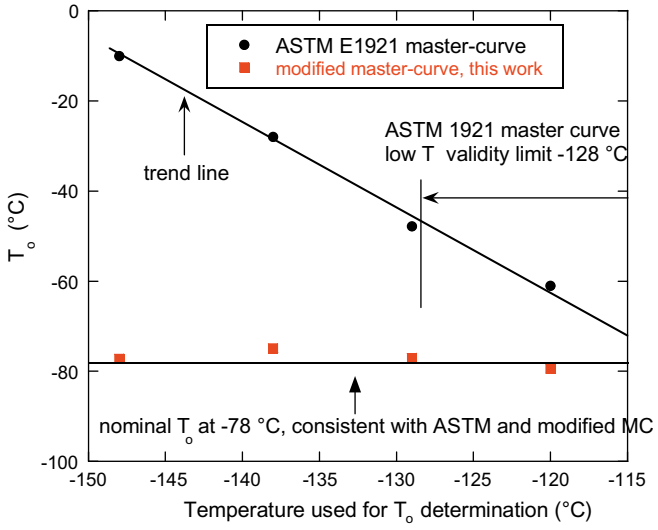

Fig. 4. Single temperature T_o determination versus testing temperature with the ASTM-MC and modified MC.

single temperature determination made on the four lower temperature datasets. As indicated in Fig. 4, the two lowest temperature datasets are well outside the validity range of the ASTM E1921 applicability range, the dataset at −129 °C is just 1 °C out and the dataset at −120 °C is within the applicability range. T_o determinations out the applicability temperature range of the ASTM E1921 standard were done to find how fast T_o diverges from the correct value when analyzing data at temperature lower than T_o −50 °C. The trend line showed in Fig. 4 indicates that T_o decreases with increasing T_o determination temperature indicating that on the lower shelf side, the ASTM master-curve does not describe properly the median toughness, even in the temperature range where it is supposed to work. Indeed, applying the ASTM E1921 standard at −128 and −120 °C, the trend line in Fig. 4 indicates that testing at those last temperatures would yield T_o values, respectively, 30 and 15 °C greater than the correct T_o. In addition, it is emphasized that the T_o values calculated on the low temperature datasets are very far from the T_o value calculated on the 0.87T $C(T)$ data, which is −78 °C; they overestimate T_o determined with the 0.87T $C(T)$ specimens up to about 50 °C. These observations, made possible by the large number of data points in this analyzed database, led us to make an adjustment of the toughness–temperature curve shape.

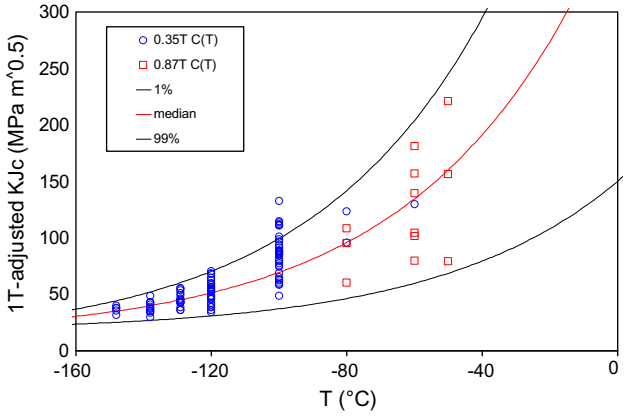

Fig. 5. Modified master-curve analysis on the 0.87T $C(T)$ data, T_o = −78 °C.

Table 1
Statistics on the fully constrained datasets (see text) calculated with the ASTM E1921 master-curve, T_o = −78 °C.

Lower bound: LB (%)	Data below LB	Upper bound: UB (%)	Data above UB	Total data out of the two bounds	Expected data out of the two bounds
5	14	95	1	15	7
10	26	90	1	27	14
20	40	80	2	42	28
35	53	65	6	59	49

Table 2
Statistics on the fully constrained datasets (see text) calculated with the modified master-curve Eq. (9). A = 12 MPa m$^{1/2}$, T_o = −78 °C.

Lower bound: LB (%)	Data below LB	Upper bound: UB (%)	Data above UB	Total data out of the two bounds	Expected data out of the two bounds
5	4	95	4	8	7
10	7	90	8	15	14
20	18	80	13	31	28
35	25	65	22	47	49

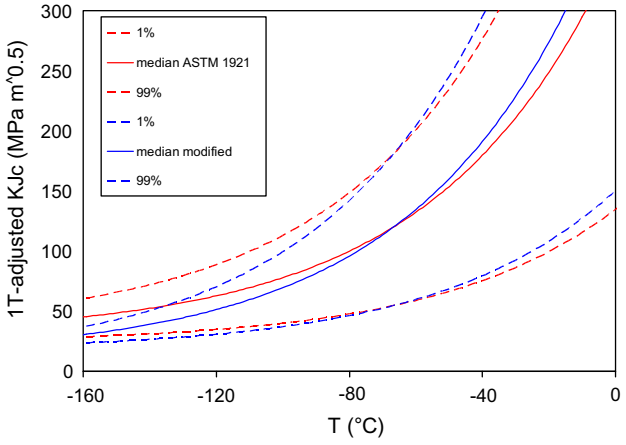

Fig. 6. Comparison of the two master-curves, note the difference in the scatter amplitude below −100 °C.

Having identified lower values of toughness than predicted by the ASTM E1921 master-curve, an adjustment of the coefficients in Eq. (6) was done. While it is in principle possible to fit the three parameters (A, C and T_o), we followed the procedure recommended by Wallin [20] and fitted only the athermal part of the master-curve (A) and the reference temperature T_o. This approach allows improving the description of the toughness–temperature curve in the lower transition region without modifying appreciably the general properties of the master-curve in the middle transition region [21]. The two coefficients were then obtained by solving numerically and iteratively Eqs. (8a) and (8c). As mentioned at the end of the first paragraph of this section, we emphasize that we have considered only the fully constrained datasets. For example, the data of the 0.35T $C(T)$ at −100 °C were not included in the shape assessment as the cumulative failure probability function of these data was shown to be biased by constraint loss. The resolution of the system of equations yielded the following parameters for the so-called modified master-curve:

$$K_{Jc\_median(1T)} = 12 + (100 - 12)\exp(0.019(T - T_o)) \quad \text{with} \quad T_o = -78\ ^\circ\text{C}. \tag{9}$$

This modified master-curve is plotted in Fig. 5 where we can show that on the lower shelf side, the curve describes much better the data. Note that the data above the 99% failure bound at −100 °C are believed to have suffered from constraint loss. Using a calibrated local criterion for quasi-cleavage, see for instance in [3,11,12], it would possible to constraint correct those points but no attempt to do so has been done in the framework of this study. In order to cross-check the self-consistency of the modified master-curve, we performed a second multi-temperature T_o determination of the 0.87T $C(T)$ data only and found T_o = −75 °C, which is in good agreement with the T_o obtained in Eq. (9), whose parameters are somewhat overweighed by the many low temperature data points. We also recalculated T_o with the modified master-curve equation on the low temperature 0.35T $C(T)$ datasets and plotted the results in Fig. 4. While a very weak decrease of T_o was found (red[1] squares) the absolute value of T_o is now consistent with a nominal T_o at −78 °C.

A check of the statistical description of the database (fully constrained datasets, namely those at −148, −138, −129, −120, −80, −60 °C), which contains 70 points, was done for the modified master-curve and compared with the ASTM E1921 master-curve. By combining Eq. (2) with Eq. (5), it is straightforward to derive the temperature dependence on any given cumulative failure probability X, which is then given by

$$K_{Jc(X)} = K_{\min} + \left[\ln\left(\frac{1}{1-X}\right)\right]^{1/4} \times \left\{\frac{A - K_{\min}}{\ln(2)^{1/4}} + \frac{(100 - A)}{\ln(2)^{1/4}}\exp[0.019(T - T_o)]\right\}. \tag{10}$$

In Tables 1 and 2, we counted the number of points falling above the upper bound and below the lower bound, determined with Eq. (10) for the desired failure probability and we compared the results with the predicted number. Again, we observe that the number of points falling out the bounds is completely asymmetric for the ASTM master-curve (Table 1) and inconsistent with the predictions when the master-curve and associated bounds are extended to lower temperatures than T_o −35 °C, i.e. even in the valid temperature range. On the contrary, a very good agreement was found for the modified master-curve (Table 2).

We emphasize that the modifications in the master-curve shape we propose here are critical if T_o determination is foreseen in a temperature window close to T_o −50 °C while they are almost irrelevant if T_o is determined with 1T-thick specimens at temperature close to T_o. This is illustrated in Fig. 6 where the two master-curves are plotted together. Clearly, one can see that below −120 °C the amplitude of the scatter of the modified master-curve lies between the lower bound and median curve of the

[1] For interpretation of color in Fig. 4, the reader is referred to the web version of this article.

ASTM master-curve. Note that the ASTM E1921 procedure does not recommend doing crack front length adjustments of toughness (Eq. (3)) near the lower shelf. However, if the crack front adjustments are not done on the datasets at −148 and −138 °C, which contain 17 data, 16 data remain below the ASTM E1921 median master-curve. This observation gives additional credit to a moderate adjustment of the athermal component of the master-curve. The value of the athermal component in Eq. (9) (12 MPa $m^{1/2}$) suggests that the K_{min} value in Eq. (2) may be lower than 20 MPa $m^{1/2}$. Work is currently in progress to better assess the overall fracture toughness behavior on the lower shelf. Having to assess fracture toughness before and after irradiation with small specimens prone to very rapid constraint loss, it is critical to know precisely the toughness–temperature behavior close to the lower shelf to predict correctly T_o by extrapolation of the $K_{Jc\_med}(T)$ equation.

5. Conclusions

The fracture toughness behavior of the Eurofer97 steel was investigated in the lower to middle ductile to brittle transition region. From a comparison of the failure probability diagrams of two different specimen sizes, we concluded that constraint loss begins at rather low deformation level, characterized by M of about 80, while the ASTM E1921 standard recommends $M = 30$. By determining T_o in the middle transition region with the 0.87T $C(T)$ specimens, we showed that in the lower transition region, the ASTM E1921 master-curve does not predict satisfactorily the temperature dependence of the median toughness and the scatter. In order to improve the description of the data near the lower shelf region, two parameters of the master-curve were fitted using the method of maximum likelihood, namely the athermal component, A, and the reference temperature, T_o. We found that the athermal part is significantly lower (12 MPa $m^{1/2}$) than the recommended value of the ASTM E1921 master-curve (30 MPa $m^{1/2}$). Thanks to the adjustment of the coefficient A, we demonstrated that the modified master-curve allows determining accurately T_o from tests at temperatures near the lower shelf region. Indeed, a value of T_o was found almost independent of the dataset temperature used to determine it when using the single temperature T_o determination method. Therefore, it is of primary importance not to overlook such shape adjustment if small specimens are used near the lower shelf to determine T_o.

Acknowledgements

The financial support of the Swiss National Foundation is gratefully acknowledged. This work, supported by the European Communities under the contract of Association between EURATOM/(Switzerland), was carried out within the framework of the European Fusion Development Agreement (EFDA). The views and opinions expressed herein do not necessarily reflect those of the European Commission. The Paul Scherrer Institute is acknowledged for providing access to its facility. J.-W. Rensman and E. Lucon are gratefully thanked for fruitful discussion of the manuscript.

References

[1] R.L. Klueh, D.R. Harris, High-Chromium Ferritic and Martensitic Steels for Nuclear Applications, ASTM, West Conshohocken, PA, 2001.
[2] J. Rensman, J. van Hoepen, J.B.M. Bakker, R. den Boef, F.P. van den Broek, E.D.L. van Essen, J. Nucl. Mater. 307–311 (2002) 245.
[3] G.R. Odette, T. Yamamoto, H.J. Rathbun, M.Y. He, M.L. Hribernik, J.W. Rensman, J. Nucl. Mater. 323 (2003) 313.
[4] M.A. Sokolov, R.L. Klueh, G.R. Odette, K. Shiba, H. Tanigawa, in: M.L. Grossbeck, T.R. Allen, R.G. Lott, A.S. Kumar (Eds.), Effects of Radiation on Materials, ASTM STP 1447, West Conshohoken, PA, 2004, p. 408.
[5] K. Shiba, M. Enoeda, S. Jitsukawa, J. Nucl. Mater. 329–333 (2004) 243.
[6] T. Yamamoto, G.R. Odette, D. Gragg, H. Kurishita, H. Matsui, W.J. Yang, M. Narui, M. Yamazaki, J. Nucl. Mater. 367–370 (2007) 593.
[7] P. Spätig, R. Bonadé, G.R. Odette, J.W. Rensman, N. Campitelli, P. Mueller, J. Nucl. Mater. 367–370 (2007) 527.
[8] G.R. Odette, K. Edsinger, G.E. Lucas, E. Donahue, in: W.R. Corwin, S.T. Rosinski, E. van Walle (Eds.), Small Specimen Test Techniques, ASTM STP 1329, American Society for Testing and Materials, 1998, p. 298.
[9] G.R. Odette, M.Y. He, J. Nucl. Mater. 283–287 (2000) 560.
[10] Standard Test Method for Determination of Reference Temperature, T_o, for Ferritic Steels in the Transition Range, E1921, Annual Book of ASTM Standards 2004, vol. 03.01, ASTM International, 2004.
[11] G.R. Odette, T. Yamamoto, H. Kishimoto, M. Sokolov, P. Spätig, W.J. Yang, J.W. Rensman, G.E. Lucas, J. Nucl. Mater. 329–333 (2004) 1243.
[12] R. Bonadé, P. Mueller, P. Spätig, Eng. Fract. Mech. (2008), doi:10.1016/j.engfracmech.2008.01.016.
[13] E. Lucon, J. Nucl. Mater. 367–370 (2007) 575.
[14] K. Wallin, Eng. Fract. Mech. 19 (6) (1984) 1085.
[15] K. Wallin, J. Phys. IV, Coll. C7 Suppl. J. Phys. III 3 (1993) 575.
[16] H.J. Rathbun, G.R. Odette, M.Y. He, T. Yamamoto, Eng. Fract. Mech. 73 (2006) 2723.
[17] K. Wallin, Int. J. Press. Ves. Piping 55 (1993) 61.
[18] R. Bonadé, P. Spätig, N. Baluc, J. Nucl. Mater. 367–370 (2007) 581.
[19] C. Lipton, N.J. Sheth, Statistical Design and Analysis of Engineering Experiments, McGraw-Hill, New York, 1973.
[20] K. Wallin, in: Recent Advances in Fracture (Proceedings of the International Conference) Minerals, Metals and Materials Society, Warrendale, PA, 1997, p. 171.
[21] IAEA Technical Reports Series No. 429, Guidelines for Application of the Master Curve Approach to Reactor Pressure Vessel Integrity in Nuclear Power Plants, IAEA, Vienna, 2005.